

# Polymer Chemistry

Volume 16  
Number 15  
21 April 2025  
Pages 1621-1724

rsc.li/polymers



ISSN 1759-9962

 ROYAL SOCIETY  
OF CHEMISTRY

## PAPER

Brian Hale Northrop, Benjamin Ross Elling *et al.*  
Ring-opening metathesis polymerization of (oxa)  
norbornenes with sulfonate, sulfone, and sulfoxide  
sidechains

**15**  
YEARS  
ANNIVERSARY

Cite this: *Polym. Chem.*, 2025, **16**, 1653

# Ring-opening metathesis polymerization of (oxa) norbornenes with sulfonate, sulfone, and sulfoxide sidechains†

Oliver Paul Clarke,<sup>‡</sup> Abdulrahman Bashir,<sup>†</sup> Sophie Wazłowski, Sara Ptaszynska, Brian Hale Northrop<sup>\*</sup> and Benjamin Ross Elling<sup>\*</sup>

Sulphur-containing polymers are utilized in applications ranging from vulcanized rubbers to optical materials and proton conducting membranes. Typically, sulphur-containing polymers are synthesized *via* condensation methods. While ring-opening metathesis polymerization is a useful tool for polymerizing functional monomers, previous reports have shown difficulties incorporating sulphur-containing functional groups due to Ru–S interactions. In this work, we report the synthesis and polymerization of a number of poly(oxa)norbornenes containing sulfonate, sulfone, and sulfoxide sidechains. We demonstrate the effects of the identity of the bridge group, sidechain R groups, and substituent stereochemistry on polymerization rates, molecular weight distributions, and thermal properties. Interestingly, while the *exo*-norbornene phenyl sulfoxide monomer was effectively polymerized, the *endo* isomer resulted in exclusive single addition to the Ru catalyst due to sulphur chelation to the metal centre. This monomer could however be used for alternating copolymerization with other cyclic olefins.

Received 17th November 2024,  
Accepted 13th March 2025

DOI: 10.1039/d4py01307g

rsc.li/polymers

## Introduction

Sulphur-containing polymers are employed in a range of commercial applications from conjugated polymers to high refractive index materials.<sup>1</sup> Since the first half of the 19<sup>th</sup> century, rubbers have been vulcanized with elemental sulphur to produce materials with controlled degrees of crosslinking and improved physical properties.<sup>2</sup> More recently, in 1962, DuPont commercialized Nafion, a perfluorinated polymer with sulfonate groups, which allow the material to be used as a proton-conducting membrane in fuel cells.<sup>3</sup> Most sulphur-containing polymers, such as polysulfones, are synthesized *via* step-growth condensation methods. However, incorporating sulphur-based functionalities into polymers *via* living chain-growth methods is desirable to control polymer molecular weight, chain-end identity, and dispersity.

Ring-opening metathesis polymerization (ROMP) is a powerful chain growth technique that is typically driven by the release of monomer ring strain. While Grubbs-type metathesis catalysts are popular due to their high functional group tolerance, some sulphur-containing functional groups have been

shown to be reactive with these Ru-based complexes. Emerik previously polymerized of a six-membered disulfide-containing monomer.<sup>4</sup> Although copolymerization with *cis*-cyclooctene was possible, the attempted homopolymerization of the disulfide monomer resulted in only oligomers, with authors finding evidence that Ru–S interactions lead to catalyst degradation. However, not all sulphur-containing functional groups are incompatible with Ru metathesis catalysts. Successful cross metathesis has been reported for vinyl sulfones and sulfoxides, suggesting acceptable compatibility with second generation Grubbs catalysts.<sup>5</sup>

We believed that, unlike sulphides, oxidized sulphur functional groups (sulfoxides, sulfones, and sulfonate esters) could be incorporated into strained cyclic olefins and polymerized without significant interaction with the catalyst Ru centre. Additionally, due to the electron-withdrawing nature of these sulphur-containing functional groups, we believed the facile synthesis of (oxa)norbornene monomers could be accomplished *via* the Diels–Alder reaction of vinyl compounds and either furan or cyclopentadiene. The ease of accessing a range of vinyl sulfones/sulphides would allow us to probe the effects of side chain identity and stereochemistry on polymerization kinetics and polymer thermal properties.

We were particularly interested in investigating the differences in metathesis behaviour between norbornene and oxanorbornene derivatives. Recent studies on oxanorbornene metathesis showed several monomers capable of single unit

Wesleyan University, Department of Chemistry, 52 Lawn Ave, Middletown, CT 06457, USA. E-mail: [belling@wesleyan.edu](mailto:belling@wesleyan.edu)

† Electronic supplementary information (ESI) available. See DOI: <https://doi.org/10.1039/d4py01307g>

‡ O.P.C and A.B. contributed equally to this work.



monomer addition (SUMI) in part due to slow oxanorbornene propagation due to oxygen coordination with the Ru centre.<sup>6</sup> Prior to these reports, only select other monomers capable of SUMI *via* ROMP have been reported.<sup>7</sup> No norbornenes derivatives have thus far shown similar SUMI. We believed careful study of a range of (oxa)norbornene monomers was warranted due to the potential discovery of new, interesting metathesis activity.

In this study, a range of new (oxa)norbornene were synthesized with sulfonate, sulfone, and sulfoxide side chains. The stereoisomers were carefully separated to investigate the polymerization of the *endo* and *exo* isomers. All (oxa)norbornenes containing sulfonate and sulfone sidechains were polymerizable, resulting in polymers with high glass transition temperatures ( $T_g$ s) with narrow molecular weight distributions (Fig. 1). However, the polymerizability of sulfoxide-containing monomers was dependent on substituent stereochemistry, with SUMI observed for the *endo* norbornene monomer.



**Fig. 1** (a) Metathesis of (oxa)norbornene monomers with sulfonate ester and sulfone side chains resulted in well controlled polymerizations; (b) metathesis of *exo*-norbornene sulfoxide resulted in polymerization with broad dispersities; (c) metathesis with the *endo*-norbornene sulfoxide monomer resulted in single unit monomer addition (SUMI).

## Results and discussion

### Synthesis of (oxa)norbornene monomers

The (oxa)norbornene monomers investigated in this study were synthesized in either one or two steps (Fig. 2a). *n*-Butyl and isopropyl vinyl sulfonates were synthesized *via* a one-pot sulfonation–elimination reaction with 2-chloroethanesulfonyl chloride, triethylamine, and the corresponding alcohol, both in excellent yields. While we attempted to synthesize the phenyl vinyl sulfonate from phenol, the product was too hydrolytically unstable to be isolated in high yield or used in the subsequent Diels–Alder reactions. Phenyl vinyl sulfone and phenyl vinyl sulfoxide were both purchased from commercial sources. These vinyl compounds were selected in order to probe the effect of the role of R group sterics on polymerization rates and polymer properties as well as the ability to incorporate a range of sulphur-based functional groups into polymers *via* ROMP.

Next, the norbornene and oxanorbornene monomers were synthesized *via* a Diels–Alder cycloaddition of the desired vinyl compound with five equivalents of cyclopentadiene or furan, respectively (Fig. 2b). The reactions were performed neat in



**Fig. 2** (a) Synthesis of vinyl sulfonate esters from 2-chloroethanesulfonyl chloride and the corresponding alcohol; (b) synthesis of (oxa)norbornene monomers *via* the Diels–Alder cycloaddition of the desired vinyl compounds and either cyclopentadiene or furan; (c) scope of monomers and catalyst used in this study.



pressure flasks at 80 °C for 24 h. The monomers used in this study (Fig. 2c) were obtained at varying degrees of conversion from the starting material (Table S1†). Quantitative conversion was obtained for all norbornene monomers synthesized with cyclopentadiene (1N, 2N, 3N, 4). However, significant amounts of vinyl starting material remained for all oxanorbornene monomer syntheses (1O, 2O, 3O). In particular, the yield of 2O was low as assessed by  $^1\text{H}$  NMR analysis, with a significant amount of insoluble black material collected when following the standard reaction and negligible monomer isolated following silica gel chromatography. However, enough 2O was isolated after the reaction was performed using a fifty-fold excess of furan.

We also quantified the *exo/endo* stereoisomer ratio *via* analysis of the crude  $^1\text{H}$  NMR spectra, using the characteristic coupling constants (as predicted by the Karplus equation) to inform our isomer identification.<sup>8</sup> For the norbornene monomers, major product was the *endo* isomer, as would be expected for a classical Diels–Alder system operating under kinetic control.<sup>9</sup> Interestingly, for the furan monomers, the major product was instead the *exo* isomer.

To examine the factors that underlie both the different extents of conversion and the different composition of stereoisomers, we performed a DFT study mapping out relative transition state and product free energies for *exo* and *endo* stereoisomers originating from cyclopentadiene and from furan. Calculations were performed at the M06-2x/6-31G(d) level, which has been shown to agree well with experimental activation parameters of Diels–Alder reactions.<sup>10</sup> Given the similar conversions and product distributions for the range of monomers used in this study, we narrowed our focus to only the cycloaddition of phenyl vinyl sulfone with either cyclopentadiene or furan. Key insights from computational analysis are summarized in Fig. 3. In the case of cyclopentadiene reacting with phenyl vinyl sulfone (Fig. 3a) the *exo/endo* ratio is kinetically driven given that product formation is significantly exergonic ( $-\Delta G^\circ = 19.3\text{--}20.3\text{ kcal mol}^{-1}$ ) such that the reverse Diels–Alder reaction is kinetically prohibitive. Computations predict an *exo/endo* ratio of 30:70, which is consistent with the experimental ratio of 34:66. Furthermore, the large thermodynamic driving force and relatively low free energy barriers ( $\Delta G^\ddagger = 21.9\text{--}22.4\text{ kcal mol}^{-1}$ ) support the experimentally observed high conversion of norbornene derivatives.

Computational modelling of the reactivity between phenyl vinyl sulfone reacts and furan (Fig. 3b) predicts the oxanorbornene product formation to be exergonic, but only slightly, with *exo* and *endo* free energies of  $-2.0$  and  $-2.1\text{ kcal mol}^{-1}$ , respectively. Free energy barriers are found to be  $\sim 4\text{--}5\text{ kcal mol}^{-1}$  higher than for the same reaction with cyclopentadiene. Given the low predicted thermodynamic driving force and moderate transition state barriers, the Diels–Alder reaction with furan is predicted to be under thermodynamic control. The calculated *exo/endo* ratio of 46:54 is consistent, within error, of the experimentally measured ratio of 58:42.

To carefully examine the effects of side chain stereochemistry on polymerization and material properties, we care-

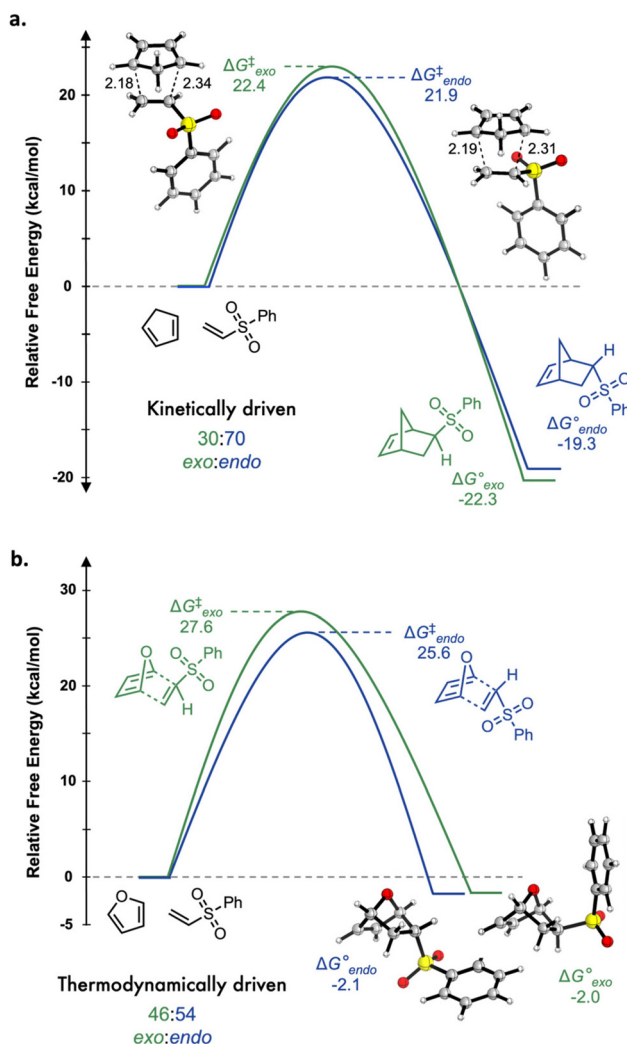


Fig. 3 Potential energy diagrams of the reaction of phenyl vinyl sulfone with either (a) cyclopentadiene or (b) furan.

fully separated the two stereoisomers *via* flash chromatography on silica gel. In all cases, we found that the first isomers to elute were the *endo* stereoisomers. Given similar overall polarities of the molecules, significant coelution was often observed. In these cases, small fractions were collected to ensure.

### Propagation kinetics

Having obtained pure stereoisomers monomers of each (oxa) norbornene, we studied the propagation kinetics when the monomers were polymerized with Grubbs fast initiating catalyst (G3). Previous studies have examined the propagation of other *endo/exo* norbornene derivatives.<sup>11</sup> A stock solution of G3 in  $\text{CDCl}_3$  was prepared and 1 equiv. of G3 was added to 100 equiv. of monomer in a sealed NMR tube under an atmosphere of nitrogen.  $^1\text{H}$  NMR spectra of the solution were acquired over a range of timepoints to observe the monomer conversion to polymer. The relationship between  $\ln[M/M_0]$  and



time was linear, suggesting fast initiation and a well-controlled polymerization. The pseudo first-order rate constants for the polymerization of these monomers are shown in Table 1.

In comparing the rate constants of these monomers, a few distinct trends emerged. In all cases, the norbornenes had greater propagation rate constants than the corresponding oxanorbornenes, a phenomenon that has been previously reported.<sup>12</sup> The origins of this behaviour have not fully been investigated, perhaps due to the formation of an oxygen chelate with the Ru centre. Additionally, the *exo* isomers polymerized at a faster rate than the *endo* isomers. While the Grubbs catalyst is thought to exhibit preferential binding to the *exo* face of the monomer, the decreased reaction rates of *endo*-substituted monomers is thought to be due to the significant strain in *endo*-substituted monomers will result upon formation of the metallacyclobutane intermediate.<sup>13</sup>

The comparisons between the propagation rates and R group were particularly interesting. Looking at the *exo*-norbornene isomers of **1N**, **2N**, and **3N**, as the R group was changed from OnBu to OiPr to Ph, the propagation rate constant increased from 26.4 M<sup>-1</sup> s<sup>-1</sup> to 35.6 M<sup>-1</sup> s<sup>-1</sup>. Conversely, for the *endo*-norbornene isomers, the rate decreased from 8.4 M<sup>-1</sup> s<sup>-1</sup> to 1.8 M<sup>-1</sup> s<sup>-1</sup>. This suggested that the *endo* monomer polymerization rates larger sterics significantly slowed propagation. For **endo-3N**, arene–Ru interactions could have resulted in the slowed reaction.<sup>14</sup> Conversely, for the *exo*-isomers, the larger R groups could result in less interaction between the electronegative side-chain atoms and the Ru centre. Originally, a phenyl sulfonate monomer had been targeted, but the hydrolytic instability made it impossible to isolate. When looking at the oxanorbornene derivatives, a similar trend was observed.

Finally, we investigated the polymerization of the sulfoxide monomer **4**. **exo-4** was polymerizable, albeit at a slow rate, with a rate constant of 2.8 M<sup>-1</sup> s<sup>-1</sup>. However, upon attempting the same kinetics study with **endo-4**, no observable conversion was observed. We additionally attempted to polymerize **endo-4**

with a monomer to **G3** ratio of 10 : 1. After 24 h, only 9% conversion was observed *via* <sup>1</sup>H NMR spectroscopy (Fig. S1†). This suggested that after initial ring opening, the S–Ru chelation prevented further polymerization, resulting in monomer single addition to the catalyst. To support our hypothesis that this S–Ru was the primary cause of this slow reactivity, we synthesized ketone analogue **endo-5**. While this polymer showed slow propagation, it nevertheless polymerized with a rate constant of 2.6 kcal mol<sup>-1</sup>.

### Polymer properties

All monomers were next polymerized with a monomer : **G3** ratio of 100 : 1 in CHCl<sub>3</sub> for 30 min to ensure complete conversion. Polymerization was terminated following the addition of excess ethyl vinyl ether, and polymers were precipitated out of methanol. The polymer samples were then subjected to gel-permeation chromatography (GPC) analysis with DMF as the mobile phase to investigate the samples' molecular weights and dispersities (Table 2). Most of the samples were not soluble in THF.

While all polymers had  $M_{n, GPC}$  that varied greatly from their predicted theoretical  $M_n$ , this was largely owed due to the reliance on polymethyl methacrylate (PMMA) standards as opposed to more values from multi-angle static light scattering. For all sulfonate and sulfone monomers, the molecular weight dispersities were rather low, typically below 1.1. The one exception was poly(**endo-2N**), with a  $D$  of 1.19. Interestingly, this was the same monomer that was shown to have a refractory period before significant propagation as observed, suggesting the increased dispersity may have been from slow initiation.

Table 2 GPC and DSC analysis for homopolymers and copolymers

Monomer	Comonomer	$M_{n, theo}^c$ (kDa)	$M_{n, GPC}^d$ (kDa)	$D^d$	$T_g^e$ (°C)
<b>exo-1N</b> <sup>a</sup>	—	23.0	97.0	1.06	178
<b>endo-1N</b> <sup>a</sup>	—	23.0	49.4	1.03	175
<b>exo-1O</b> <sup>a</sup>	—	23.2	51.6	1.04	186
<b>endo-1O</b> <sup>a</sup>	—	23.2	115.1	1.09	178
<b>exo-2N</b> <sup>a</sup>	—	21.6	41.6	1.12	174
<b>endo-2N</b> <sup>a</sup>	—	21.6	44.7	1.19	177
<b>exo-2O</b> <sup>a</sup>	—	21.8	65.2	1.07	196
<b>endo-2O</b> <sup>a</sup>	—	21.8	71.2	1.07	206
<b>exo-3N</b> <sup>a</sup>	—	23.4	56.8	1.03	192
<b>endo-3N</b> <sup>a</sup>	—	23.4	57.8	1.04	182
<b>exo-3O</b> <sup>a</sup>	—	23.6	54.2	1.12	180
<b>endo-3O</b> <sup>a</sup>	—	23.6	42.4	1.10	187
<b>exo-4</b> <sup>a</sup>	—	21.8	24.9	1.44	170
<b>endo-5</b> <sup>a</sup>	—	19.8	27.6	1.08	173
<b>endo-4</b> <sup>b</sup>	CPen	32.9	12.3	1.34	164
<b>endo-4</b> <sup>b</sup>	COct	28.6	14.4	1.30	165

<sup>a</sup> Reaction conditions: CDCl<sub>3</sub>, [M]<sub>0</sub>/[G3]<sub>0</sub> = 100, 30 min. <sup>b</sup> Reaction conditions: CDCl<sub>3</sub>, [M]<sub>0</sub>/[G3]<sub>0</sub> = 100, [M]<sub>0</sub> : comonomer 1 : 2, 24 h. <sup>c</sup>  $M_{n, theo}$  calculated assuming complete **G3** initiation and quantitative monomer conversion. <sup>d</sup> GPC analysis performed in DMF with PMMA calibrants used to determine  $M_{n, GPC}$  and  $D$ . <sup>e</sup>  $T_g$  determined using transition observed on second heating.

Table 1 First-order propagation kinetics

Monomer	Stereoisomer	Rate constant <sup>a</sup> (M <sup>-1</sup> s <sup>-1</sup> )
<b>1N</b>	<i>exo</i>	24.8 ± 3.4 <sup>b</sup>
	<i>endo</i>	8.0 ± 3.5 <sup>b</sup>
<b>1O</b>	<i>exo</i>	4.2
	<i>endo</i>	2.5
<b>2N</b>	<i>exo</i>	27.2
	<i>endo</i>	10.6
<b>2O</b>	<i>exo</i>	5.0
	<i>endo</i>	2.0
<b>3N</b>	<i>exo</i>	35.6
	<i>endo</i>	1.8
<b>3O</b>	<i>exo</i>	19.5
	<i>endo</i>	0.4
<b>4</b>	<i>exo</i>	2.8
	<i>endo</i>	—
<b>5</b>	<i>endo</i>	2.6

<sup>a</sup> Reaction conditions: CDCl<sub>3</sub>, [M]<sub>0</sub>/[G3]<sub>0</sub> = 100. <sup>b</sup> Kinetics experiments performed in quadruplicate. The rate constant is the average of the four experiments, with the error the standard deviation.



Additionally, we investigated the thermal properties of these samples *via* differential scanning calorimetry (DSC). All samples displayed only one second-order thermal transition corresponding to the glass-transition temperature ( $T_g$ ) at high temperatures  $>170$  °C. Interestingly, no consistent relationship between the bridgehead group identity or stereochemistry and  $T_g$  were noticed. Unsurprisingly, the larger  $-OiPr$  and  $-Ph$  R groups resulted in polymers with slightly higher  $T_g$ s than the polymers with the more flexible, linear  $-OnBu$  side chains. The difference between the lowest and highest  $T_g$ s for all polymer samples was 42 °C.

#### Alternating polymerization with *endo-4*

Finally, we sought test if the poor propagation of *endo-4* could instead be used to synthesize alternating polymers with cyclic olefins cyclopentene (**CPen**) and cyclooctene (**COct**). While both **CPen** and **COct** are capable of homopolymerization at appropriately high concentrations, we hypothesized that the higher strain of *endo-4* that results in single addition would result in rigorous alternation. Following ring opening, the S–Ru chelation would prevent further polymerization of the sterically demanding *endo-4*. However, upon ring opening of **CPen** or **COct**, a new *endo-4* would coordinate and ring open. Copolymerization of *endo-4* with either **CPen** or **COct** was attempted at 1 M overall in monomer, with *endo-4* to cyclic olefin ratio of 1 : 2. The copolymerization of *endo-4* with both **CPen** and **COct** was particularly slow, with after 24 h only 10% and 18% conversion, respectively, as observed by  $^1H$  NMR spectroscopy (Fig. S2 and S3<sup>†</sup>). While due to the low conversions and poor solubility of *endo-4* in MeOH made full characterization of the copolymers impossible, an analysis of the  $^1H$  NMR spectra showed a roughly 1 : 1 incorporation of both monomers despite the greater monocyclic olefin in solution, suggesting highly rigorous alternation at least at low conversion. Neither *endo-4* nor **CPen** are homopolymerizable at an initial concentration of 0.05 M, with **CPen**'s critical equilibrium concentration at 25 °C  $> 0.8$  M.<sup>15</sup> To be sure, metathesis below the equilibrium concentration does not preclude the possibility of several additions of **CPen**.<sup>16</sup> However, the similar incorporation of both **CPen** and **COct** despite **COct** having an equilibrium concentration  $>0.05$  M suggests significant alternation.<sup>17</sup> Studies are ongoing to better characterize the single-addition nature of *endo-4* and to quantify its degree of alternation with lower-strain cyclic olefins.

The GPC traces of these samples showed low  $M_n$  values reflective of the low conversion. The dispersities  $\sim 1.3$  suggested a broader molecular weight distribution, but interestingly a better MW control than observed with the homopolymerization of *exo-4*. The incorporation of ring-opened **CPen** and **COct** units resulted in polymers with slightly lower  $T_g$ s of 164 and 165 °C, respectively.

These data represent the first example of a norbornene monomer capable of SUMI. However, the slow kinetics of copolymerization suggest the S–Ru chelation may be too great to allow high MW copolymerization under reasonable time restrains. Synthesizing a range of sulfoxide monomers could

be a reasonable pathway for discovering other SUMI monomers with a range of polymerization kinetics.

## Conclusions

In this work, we sought to expand the scope of ROMP monomers by synthesizing (oxa)norbornene derivatives with side chains featuring sulfonate, sulfone, and sulfoxide groups. By carefully synthesizing and purifying the stereoisomers of these monomers, we were able to rigorously probe the effects of stereochemistry, bridge group identity, and R group on kinetics and polymer properties. All monomers were successfully incorporated into high molecular weight polymers with narrow molecular weight dispersities. Notably, we discovered that sulfoxide monomer *endo-4b* engaged in single addition with initiator **G3**, resulting in the alternating copolymerization of *endo-4b* with monocyclic olefins. Future investigations will focus further expanding the scope of monomers with sulfoxide side chains that may be capable of SUMI.

## Data availability

The data supporting this article, including  $^1H$  and  $^{13}C$  NMR spectra of both small molecules and polymers, GPC chromatograms, and DSC chromatograms have been included as part of the ESI.<sup>†</sup> Raw data files will be available upon request to all who inquire with the corresponding authors.

## Conflicts of interest

There are no conflicts to declare.

## Acknowledgements

The authors would like to acknowledge Elijah Kellner and the Gel Permeation Chromatography facility in Polymer Science & Engineering at the University of Massachusetts Amherst. We would also like to acknowledge the Mass Spectroscopy Facility at the University of Illinois Urbana-Champaign for collection of ESI MS data.

## References

- 1 X.-H. Zhang and P. Theato, eds, In *Sulfur-Containing Polymers*, 2021, pp. i–xxv.
- 2 M. Akiba and A. S. Hashim, *Prog. Polym. Sci.*, 1997, **22**, 475–521.
- 3 K. A. Mauritz and R. B. Moore, *Chem. Rev.*, 2004, **104**, 4535–4586.
- 4 C.-C. Chang and T. Emrick, *Macromolecules*, 2014, **47**, 1344–1350.



- 5 A. Michrowska, M. Bieniek, M. Kim, R. Klajn and K. Grela, *Tetrahedron*, 2003, **59**, 4525–4531.
- 6 (a) S. Pal, M. Alizadeh, P. Kong and A. F. M. Kilbinger, *Chem. Sci.*, 2021, **12**, 6705–6711; (b) J. C. Foster, J. T. Damron and H. Zhang, *Macromolecules*, 2023, **56**, 7931–7938.
- 7 (a) A. Song, K. A. Parker and N. S. Sampson, *J. Am. Chem. Soc.*, 2009, **131**, 3444–3445; (b) B. R. Elling and Y. Xia, *J. Am. Chem. Soc.*, 2015, **137**, 9922–9926; (c) J. K. Su, Z. Jin, R. Zhang, G. Lu, P. Liu and Y. Xia, *Angew. Chem., Int. Ed.*, 2019, **58**, 17771–17776; (d) J. K. Su, S. Y. Lee, B. R. Elling and Y. Xia, *Macromolecules*, 2020, **53**, 5833–5838.
- 8 J. H. Cooley and R. V. Williams, *J. Chem. Educ.*, 1997, **74**, 582.
- 9 J. Carneiro de Oliveira, M. P. Laborie and V. Roucoules, *Molecules*, 2020, **25**, 243.
- 10 P. Zhao, S. Hu, X. Lu and X. Zhao, *J. Org. Chem.*, 2019, **84**, 14571–14578.
- 11 (a) Y. Nishihara, Y. Inoue, Y. Nakayama, T. Shiono and K. Takagi, *Macromolecules*, 2006, **39**, 7458–7460; (b) A. B. Chang, T.-P. Lin, N. B. Thompson, S.-X. L. Luo, A. L. Liberman-Martin, H.-Y. Chen, B. Lee and R. H. Grubbs, *J. Am. Chem. Soc.*, 2017, **139**, 17683–17693; (c) M. G. Hyatt, D. J. Walsh, R. L. Lord, J. G. Andino Martinez and D. Guironnet, *J. Am. Chem. Soc.*, 2019, **141**, 17918–17925; (d) N. Miyasako, S.-i. Matsuoka and M. Suzuki, *Macromol. Rapid Commun.*, 2021, **42**, 2000326; (e) H. L. Cater, I. Balynska, M. J. Allen, B. D. Freeman and Z. A. Page, *Macromolecules*, 2022, **55**, 6671–6679.
- 12 (a) M. F. Ilker and E. B. Coughlin, *Macromolecules*, 2002, **35**, 54–58; (b) C. S. Daeffler and R. H. Grubbs, *Macromolecules*, 2013, **46**, 3288–3292; (c) M. Yasir, P. Liu, I. K. Tennie and A. F. M. Kilbinger, *Nat. Chem.*, 2019, **11**, 488–494.
- 13 W. J. Wolf, T.-P. Lin and R. H. Grubbs, *J. Am. Chem. Soc.*, 2019, **141**, 17796–17808.
- 14 E. Roth, R. V. Listyarini, T. S. Hofer and M. Cziferszky, *Inorg. Chem.*, 2024, **63**, 14021–14031.
- 15 R. Tuba and R. H. Grubbs, *Polym. Chem.*, 2013, **4**, 3959–3962.
- 16 M. Torre III, W. D. Mulhearn and R. A. Register, *Macromol. Chem. Phys.*, 2018, **219**, 1800030.
- 17 (a) A. R. Hlil, J. Balogh, S. Moncho, H.-L. Su, R. Tuba, E. N. Brothers, M. Al-Hashimi and H. S. Bazzi, *J. Polym. Sci., Part A: Polym. Chem.*, 2017, **55**, 3137–3145; (b) K. R. Sylvester, J. R. Zovinka, M. L. Milrod, A. K. Stubin, A. Rojas-Merchan, K. Alexander and B. R. Elling, *Angew. Chem., Int. Ed.*, 2025, **64**, e202414872.

